

Power dissipation mode transition by a magnetic field

S. J. You, C. W. Chung, K. H. Bai, and H. Y. Chang

Citation: *Appl. Phys. Lett.* **81**, 2529 (2002); doi: 10.1063/1.1506944

View online: <http://dx.doi.org/10.1063/1.1506944>

View Table of Contents: <http://apl.aip.org/resource/1/APPLAB/v81/i14>

Published by the [American Institute of Physics](#).

Additional information on *Appl. Phys. Lett.*

Journal Homepage: <http://apl.aip.org/>

Journal Information: http://apl.aip.org/about/about_the_journal

Top downloads: http://apl.aip.org/features/most_downloaded

Information for Authors: <http://apl.aip.org/authors>

ADVERTISEMENT



Goodfellow
metals • ceramics • polymers • composites
70,000 products
450 different materials
small quantities fast

www.goodfellowusa.com

Power dissipation mode transition by a magnetic field

S. J. You,^{a)} C. W. Chung, K. H. Bai, and H. Y. Chang

Department of Physics, Korea Advanced Institute of Science and Technology, Daejeon 305-701, South Korea

(Received 13 May 2002; accepted for publication 22 July 2002)

We measured electrical characteristics of transversely magnetized capacitively coupled plasma at low pressure (10 mTorr). From these measurements, we found that the power characteristics of the magnetized discharge were different from those of the unmagnetized discharge. As the magnetic field increases, a square dependence of power characteristic at high current changes to a linear dependence. This can be understood as a power dissipation mode transition by a magnetic field. A calculation from a simple sheath model agrees well with the experimental data. © 2002 American Institute of Physics. [DOI: 10.1063/1.1506944]

rf capacitive discharge is one of the most common reactors in semiconductor processing and many studies have been conducted in various related areas.¹⁻⁹ Much fundamental research of the capacitive discharge has found that there are many modes and their transitions in a capacitive discharge.^{1,4,6-9} Among these, the power dissipations of the discharge and their transitions were investigated by Beneking⁶ and Godyak.⁸ The capacitive discharge dissipates an rf power in two ways. One is a power dissipation by electrons in a bulk plasma, the other is a power dissipation by ions in a sheath. When a discharge current is small, electrons in the bulk plasma mainly consume the discharge power so that the discharge power is almost proportional to current ($P_{\text{dis}} \sim P_{\text{bulk}} = V_p \cdot I$). But when a discharge current is large, ions in the sheath mainly consume the discharge power so that the discharge power is almost proportional to I^2 ($P_{\text{dis}} \sim P_{\text{sheath}} = R_{\text{sh}} \cdot I^2$).⁶ Therefore, as the discharge current increases, a change of the current/power characteristic $P(I)$ from a linear to a square dependence on current is observed. This change represents the transition of power dissipation mode from electron-dominated dissipation mode to ion-dominated dissipation mode.^{8,10} There have been a few investigation into the transition of power dissipation mode.^{6,8,10} But, there have not been any studies of the magnetic field effect on the transition.

In this letter, we investigate the transverse magnetic field effect on the transition. We present an evolution of the power characteristic from a square one ($P \sim I^2$) to a linear one ($P \sim I$) as the magnetic field increases. It can be understood as an inverse transition of the aforementioned power dissipation mode transition through the magnetic field. A diffusion under the transverse magnetic field gives a clue to understanding the transition. Furthermore, through introducing an effective pressure and using the sheath resistance model in Ref. 6, we calculate the power characteristics of the magnetized capacitively discharge. The calculated result is in a good agreement with the experimental data.

The experiment is conducted in a transversely magnetized capacitively discharge reactor, as shown in Fig. 1. The reactor is asymmetrically driven at 13.56 MHz, argon, with two different size electrodes. The lower one is the grounded

electrode (200 mm) and the upper one is the powered electrode (140 mm). The two electrodes are separated by 40 mm and positioned at the center of the discharge chamber. To keep the discharge between two electrodes, a confinement ring having a diameter equal to that of the electrode and a height of 10 mm is introduced beneath the powered electrode, and each electrode is wrapped by a ceramic cylinder 200 mm in diameter and 50 mm in height. External helmholtz coils with inner diameters of 370 mm and widths of 70 mm are installed to make a dc magnetic field in the direction parallel to the electrode surface. A dc magnetic field has a uniformity within 5% up to 30 G. rf power (ENI, A1000) is delivered to the powered electrode through a standard L-type matching network and a coaxial cable. Current-voltage (I - V) measurements are performed with an I - V monitor (Scientific Systems INC, PIM) mounted on the powered electrode. The dc bias is measured at the power electrode with a high-voltage probe. In order to compare the pressure effects, experiments are performed at different pressures (from 10 to 100 mTorr).

While increasing the transverse magnetic field, we measure discharge current, voltage, and the phase between them at 10 mTorr. From these experimental data, we obtain the discharge powers and resistances with various magnetic fields, as shown in Figs. 2(a) and 2(b). The experimental data at 0 G are consistent with those of Ref. 8 which investigated the electrical characteristics of the unmagnetized capacitively discharge. As shown in Fig. 2(a), the current/power characteristic $P(I)$ at 0 G changes from a linear to a square dependence on the current. As mentioned before, this indicates a transition of power dissipation mode from an electron-dominated dissipation mode in the bulk to an ion-dominated dissipation mode in the sheath.^{6,8} Total discharge power can be expressed as

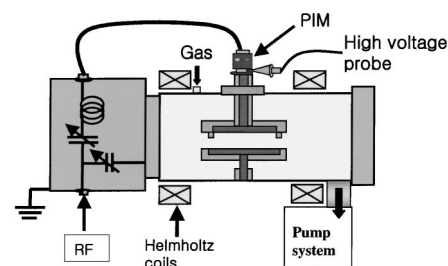


FIG. 1. Experimental setup of the transversely magnetized CCP.

^{a)}Electronic mail: spinup@cais.kaist.ac.kr

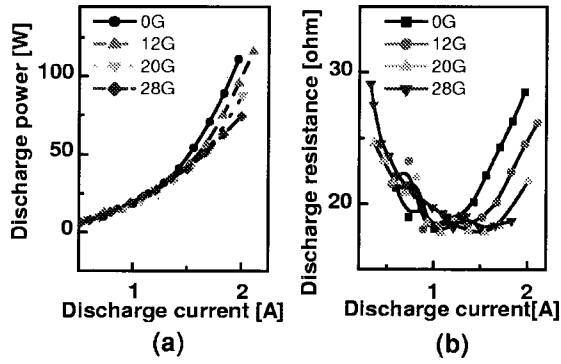


FIG. 2. Discharge power (a) and resistance characteristics (b) at 10 mTorr with various magnetic fields from the experiments.

$$P_{\text{tot}} = V_p \cdot I + R_{\text{sh}} \cdot I^2, \quad (1)$$

where I is an rf current in root-mean square (rms), V_p is an rf voltage across the bulk plasma in rms and is almost independent of current ($V_p \propto I^{-0.15}$),⁶ and the sheath resistance, R_{sh} , is a function of current and pressure. We can easily see the transition in the resistance characteristics. With increasing current, the resistance at 0 G decreases ($R_{\text{bulk}} \propto 1/I$) and reaches the minimum value and afterward increases ($R_{\text{sheath}} \propto I^{1/2}$). This also reflects the transition of power dissipation mode.⁸

However, as the magnetic field increases, the square dependence of the power characteristic at high current (~ 1.7 A) becomes smaller and almost disappears at 28 G, such that it seems to be nearly linear. It also happens in the resistance characteristics. A concave curve of resistance changes to a monotonously decreasing one as the magnetic field increases. Hence, at 28 G, there is a small power dissipation by ions, but large power dissipation by electrons. Therefore, we conclude that the magnetic field induces the transition of power dissipation mode from the ion-dominated dissipation mode to the electron-dominated dissipation mode.

To explain the transition, we consider the electron diffusion under the transverse magnetic field. The diffusion coefficient under the magnetic field can be expressed as¹¹

$$D_{\perp} = \frac{D}{1 + \omega_{ce}^2/\nu^2}, \quad (2)$$

where ν is an electron-neutral collision frequency, D ($\equiv KT/m\nu$) is a diffusion coefficient of unmagnetized plasma, and ω_{ce} ($\equiv eB/m_e$) is an electron gyrofrequency. The crossdiffusion coefficient (D_{\perp}) is reduced against the magnetic field, as in Eq. (2). The reduction of electron diffusion toward the electrode decreases the self-bias which controls the ion power dissipation in the sheath ($P_i \sim V_{\text{self}} \cdot I_i$).^{12–14} Therefore, as the magnetic field increases, the ion power dissipation in the sheath becomes smaller so that the transition of power dissipation mode finally occurs. Figure 3(a) shows the self-bias against the magnetic field at a fixed current (1.7 A). The self-bias decreases with increased magnetic field. As a result, the transition of power dissipation mode from ion-dominated dissipation to electron-dominated dissipation occurs as shown in Fig. 2.

Similarly, increasing pressure decreases the electron diffusion toward the electrode due to an increase of electron-neutral collisions ($\nu \propto P_g$), so that the self-bias also decreases against the pressure, as shown in Fig. 3(b).

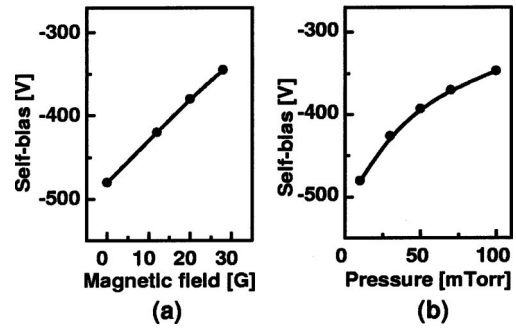


FIG. 3. Self-bias against (a) the magnetic fields and (b) the pressures at 1.7 A.

Therefore, a similar phenomenon, a power dissipation mode transition, could also be induced by a pressure, as has been observed by Godyak *et al.*⁸

As mentioned herein, the transverse magnetic field effects are similar to those of the pressure. Both decrease electron diffusion to the electrode and reduce self-bias, so that ion dissipation is reduced. Thus, we can include the magnetic field effect with a pressure effect by introducing the effective collision frequency (ν_{eff}) as

$$D_{\perp} = \frac{KT}{m\nu} \cdot \frac{1}{(1 + \omega_{ce}^2/\nu^2)} = \frac{KT}{m\nu_{\text{eff}}}, \quad (3)$$

$$\nu_{\text{eff}} \equiv \nu + \frac{\omega_{ce}^2}{\nu}. \quad (4)$$

Because the electron-neutral collision frequency is proportional to the gas pressure ($\nu \propto P_g$)¹⁶ and the electron gyrofrequency is proportional to the magnetic field ($\omega_{ce} \propto B$),¹⁵ we rewrite the expression as the effective pressure, instead of the effective collision frequency:

$$P_{\text{eff}} \approx P_g + \alpha \cdot \frac{B^2}{P_g}, \quad (5)$$

where P_g is gas pressure (mTorr), B is a magnetic field (G), and $\alpha \approx 0.83$ (mTorr²/G²) is constant.

To theoretically calculate the magnetic field effect to the transition with the effective pressure, we should get the R_{sh} expression as a function of the pressure and current. This has been theoretically investigated by Beneking for an unmagnetized discharge.⁶ Because the electron density in the sheath is so small, the sheath resistance represents the space-charge limited ion current resistance in the sheath. The resistance can be expressed as⁶

$$R_{\text{sh}} = (\sqrt{2})^{5/2} \left(\frac{5}{3\epsilon_0 A} \right)^{3/2} \cdot \left(\frac{2k}{3\sqrt{P_g}} \right) \frac{\sqrt{I}}{\omega^{5/2}}, \quad (6)$$

where I is an rms rf current, ω is a driving frequency, A is an electrode area, k ($\equiv 103.75m^{3/2}Pa^{1/2}/V^{1/2}S$) is mobility constant and P_g is a gas pressure.

It is noticeable that R_{sh} depends only on external parameters, such as A , k , P_g , I , and ω . Although this expression is derived under collisional sheath regime, it is well known that resistance dependence of current and pressure $R_{\text{sh}} \propto \sqrt{I/P_g}$ agrees well with experimental data for all range of gas pressures.^{8,14}

We obtain total discharge power by substituting Eq. (5) into Eq. (6) instead of P_g and substituting the result into Eq. (1)

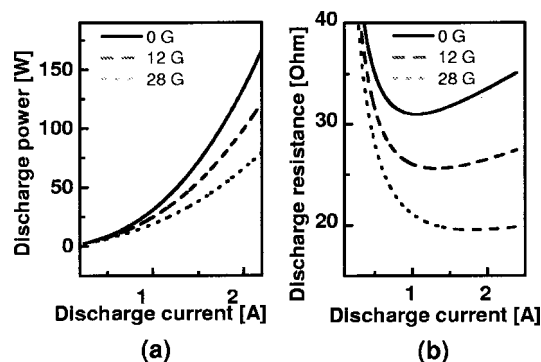


FIG. 4. Discharge power (a) and resistance characteristics (b) at 10 mTorr with various magnetic fields from the calculation of Eq. (7).

$$P_{\text{tot}} = V_p \cdot I + (\sqrt{2})^{5/2} \left(\frac{5}{3\epsilon_0 A} \right)^{3/2} \cdot \left(\frac{2k}{3 \cdot 2.73 \sqrt{P_g + \alpha \cdot B^2 / P_g}} \right) \left(\frac{I}{\omega} \right)^{5/2}, \quad (7)$$

where 2.73 is introduced through a pressure unit change from Pascal to mTorr. $V_p \approx 12$ is experimentally determined by measuring the slope of the power characteristic curve at low current. It is noted that V_p is almost constant against the magnetic field.

Figure 4 shows the calculated result of Eq. (7) for $A = 1.5 \times 10^{-2} \text{ m}^2$, $V_p \approx 12 \text{ V}$, $\omega = 2\pi \times 13.56 \times 10^6 \text{ Hz}$, $\alpha \approx 0.83 \text{ mTorr}^2/\text{G}^2$. As shown in Figs. 2 and 4, the calculated results are qualitatively consistent with the experimental results. As the magnetic field increases, the power characteristic [$P(I)$] changes from a square dependence to a linear dependence, and the resistance changes from a concave curve to a monotonously decreasing curve. However, there is a discrepancy between the experimental and the calculated results, as shown in Figs. 2 and 4. The experimentally obtained resistance is a less strong function of the magnetic field, compared with the calculated resistance. It could be understood by considering the $\mathbf{E} \times \mathbf{B}$ drift expected effect in a magnetized capacitively coupled plasma (CCP).^{17,18} The drift causes a plasma shift in the direction of $\mathbf{E} \times \mathbf{B}$,¹⁸ thus reducing the electrode area (A) in Eq. (7). The decreased area increases sheath resistance and it has an opposite effect on the effective pressure increase. Therefore, the experimental result of the resistance seemed to be a less strong function of the magnetic field than the calculated resistance.

Figure 5 shows the characteristics of the power and resistance at 0 G and 100 mTorr. The characteristics at 100 mTorr are very similar to those of the magnetized discharge (28 G) at low pressure (10 mTorr). This is evidence that the transition of the power dissipation mode is mainly induced by the effective pressure (gas pressure + magnetic field).

Compared with other magnetized discharge models,^{13,14} ion dissipation power is proportional to B^{-1} in our model while B^{-2} in other models. Although Eq. (7) does not include an electron power dissipation in the sheath investigated in Ref. 19, the calculated current/power characteristics are qualitatively well consistent with our experimental data and other published data.^{8,10,19}

In conclusion, through electrical measurements of the capacitive discharge in various magnetic fields, we observed

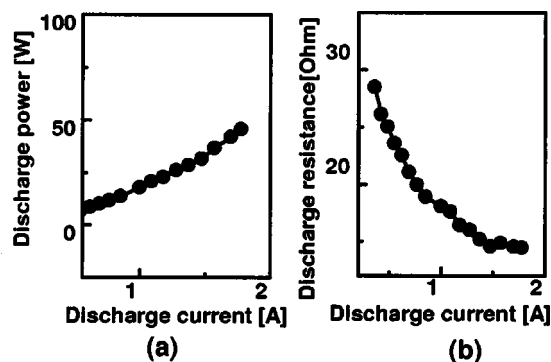


FIG. 5. Discharge power (a) and resistance characteristics (b) at 100 mTorr, 0 G from the experiments.

the transition of power dissipation mode at high current by a magnetic field. Because a magnetic field decreases the self-bias and the ion dissipation in the sheath, the power dissipation mode transition takes place from ion-dominated power dissipation to electron-dominated power dissipation, as the magnetic field increases. Through introducing the effective pressure, we include the magnetic field effect with a pressure effect, and with the Beneking sheath model including the effective pressure, we could theoretically evaluate the transition.

This work was sponsored in part by the SYSTEM I.C. 2010 of Ministry of Science and Technology (MOST) and Ministry of Commerce, Industry, and Energy (MOCIE), and by a grant from the Interdisciplinary Research Program of the KOSEF. This work is also supported by National Research Laboratory Project of Korea. One of authors thanks PLASMA, Inc. for technical and financial support for this work.

¹ Y. Catherin, C. R. Acad. Sci B. **273**, 4 (1971).

² B. Chapman, *Glow Discharge Process* (Wiley, New York, 1980).

³ K. Takaki, D. Taguchi, and T. Fujiwara, Appl. Phys. Lett. **78**, 2646 (2001).

⁴ V. A. Godyak, R. B. Piejak, and B. M. Alexandrovich, Phys. Rev. Lett. **68**, 1 (1992).

⁵ S. V. Berezhnoi, I. K. Kanganovich, and L. D. Tsendin, Plasma Phys. Rep. **24**, 7 (1998).

⁶ C. Beneking, J. Appl. Phys. **68**, 1 (1990).

⁷ V. A. Godyak, R. B. Piejak, and B. M. Alexandrovich, Plasma Sources Sci. Technol. **1**, 36 (1992).

⁸ V. A. Godyak, R. B. Piejak, and B. M. Alexandrovich, IEEE Trans. Plasma Sci. **19**, 4 (1991).

⁹ M. M. Turner, D. A. W. Hutchinson, R. A. Doyle, and M. B. Hopkins, Phys. Rev. Lett. **76**, 12 (1996).

¹⁰ V. A. Godyak, P. B. Piejak, and B. M. Alexandrovich, J. Appl. Phys. **69**, 3455 (1991).

¹¹ F. F. Chen, *Introduction to Plasma Physics and Controlled Fusion* (Plenum, New York, 1980), p. 171.

¹² Y. Li, A. Lizudk, and N. Sato, Nucl. Instrum. Methods Phys. Res. B **132**, 585 (1997).

¹³ M. A. Lieberman, A. J. Lichtenberg, and S. E. Savas, IEEE Trans. Plasma Sci. **19**, 2 (1991).

¹⁴ J. C. Park and B. K. Kang, IEEE Trans. Plasma Sci. **25**, 3 (1997).

¹⁵ M. A. Lieberman and A. J. Lichtenberg, *Principles of Plasma Discharges and Materials processing* (Wiley, New York), p. 87.

¹⁶ S. C. Brown, *Basic Data of Plasma Physics* (Wiley, New York, 1994), pp. 3, 65.

¹⁷ H. C. Shin, K. Noguchi, X. Y. Qian, N. Jha, G. Hills, and C. Hu, IEEE Electron Device Lett. **14**, 2 (1993).

¹⁸ S. Nakagkwa, T. Sasaki, H. Mori, and T. Namura, Jpn. J. Appl. Phys., Part 1 **33**, 2194 (1994).

¹⁹ K. E. Orlov and A. S. Smirnov, Plasma Sources Sci. Technol. **2**, 273 (1993).